Iranian Journal of Electrical and Electronic Engineering

Journal Homepage: ijeee.iust.ac.ir

4-18 GHz Zero-Bias Asymmetrical Spacer Layer Tunnel Diode Detector

Omar S. Abdulwahid*(C.A.), Saad G. Muttlak**, J. Sexton***, M.J. Kelly****, Mohamed Missous***

Abstract: An analysis of 6×6 μm^2 GaAs/AlAs Asymmetric Spacer Layer Tunnel diode has been conducted to evaluate the DC and RF characteristics at different bias conditions. At zero voltage operation, the diode exhibited a measured curvature coefficient of 22 V^{-1}, corresponding to a junction resistance of 27 kΩ. The measured and simulated S_{11} reflection coefficient of the integrated detector including the diode, matching circuit, and output capacitance achieved to be less than -10 dB at the desired frequency. The extracted low series resistance and junction capacitance of the tunnel diode resulted a high voltage sensitivity of 3650 V/W and low noise equivalent power of 5.5 pW/$\sqrt{Hz}$ at 11 GHz resonant frequency and -27 dBm input power. The developed detector model can be extended to implement RF detectors operating at frequencies reaching mm-wave regime applications. This is with consideration of the requirements for sub-micrometer scale mesa devices, eliminating the effects of associated parasitic elements and improved matching network performance.

Keywords: ASPAT Detector, ADS Model, Reflection Coefficient, Noise Equivalent Power.

1 Introduction

THE evolution of high-frequency RF detector is tremendously increasing due to the urgent need for commercializing various devices that are capable of sending and receiving high rate data for a range of application such as wireless communication and imaging systems [1], [2]. Other two key factors are the cost of fabrication and consumption power of these devices, especially in systems where the power capacity is limited by the available space and volume [3]. The optimization of communication systems mainly depends on the development of single integrated circuits, for instance mixers, detectors, power amplifiers, low noise amplifiers (LNA). This is incorporated with different fabrication and integration steps for the aim of minimizing RF power losses and parasitic effects [4]. RF detection is often performed in two main ways, namely coherent and incoherent approaches. The coherent technique is based on the mixing operation between RF (radio frequency) and LO (local oscillator) signal and has the benefit of providing better spectral resolution when compared to the incoherent technique. The former relies on direct detection process, typically adopted in a system array for imaging application in which the demand for low LO power and fast system response is indispensable. Furthermore, direct detectors under zero voltage bias condition find their extensive benefit in high-frequency wireless communication system as a result of the advantages of reasonable fabrication cost and low noise equivalent power (NEP) [5]. The zero-bias detector has been implemented using various structures [6], [7], [8], [9] where the forward current at a bias voltage close to zero detects the base signal associated with the RF one.

Iranian Journal of Electrical & Electronic Engineering, 2025.
Paper first received 25 Dec. 2024 and accepted 15 Jul. 2025.
* The author is with the Department of Mechatronics Engineering, College of Engineering, University of Mosul, Mosul, Iraq.
E-mail: Omar.abdulwahid@uomosul.edu.iq.
** The author is with the Department of Electrical Engineering, Tikrit University, Tikrit, Iraq.
E-mail: Saad.g.mutlak@tu.edu.iq.
*** The authors are with the Department of Electrical and Electronic Engineering, University of Manchester, Manchester, UK.
E-mails: j.sexton@manchester.ac.uk, m.missous@manchester.ac.uk.
**** The author is with the Department of Electrical Engineering, Cambridge University, Cambridge, UK.
E-mail: mjk1@eng.cam.ac.uk.
Corresponding Author: Omar S. Abdulwahid.

The use of RF detectors with high linearity and sensitivity features in receiver system can be reflected into ease the design of the low noise amplifier stage by alleviating the challenge of high gain and low noise system requirements [10], [11]. There has been extensive reported work in the literature that demonstrated Schottky detectors benefited from their great characteristics of providing high operating frequency alongside simple device layer structure and cost-effective manufacturing process [12], [13], [14]. However, voltage sensitivity of the detector devices is constrained by the maximum value of diode's curvature coefficient (K_v) as such considered a temperature dependent parameter. It can be expressed by K_v<q/kT which is the case for Schottky and Planar Doped Barrier devices [15]. Our developed tunnel structure reported in [16] and [17] mitigates this challenge through successfully achieving better temperature independence characteristics compared to the aforementioned devices with wide a range of temperature operation from -196 to 125 ℃. Moreover, the germanium tunnel diode reported in [18], exhibited higher K_v of 70 V^{-1} compared to 40 V^{-1} for Schottky structure [19]. Another parameter to consider is the junction resistance of the diode which contributes to the overall performance of the detector. A high junction resistance increases the voltage sensitivity but at the expense of complicated and narrow band matching network design. In [20], [21], [22], the Asymmetric Spacer Layer Tunnel (ASPAT) diode structure was firstly reported by Syme and Kelly as a discrete device. On-wafer measurements were performed to measure the un-matched sensitivity at only one single frequency of ~9 GHz. In [23], the on-wafer DC and RF characteristics of InGaAs and GaAs discrete ASPAT structures were demonstrated with a detailed discussion and analysis of their tunneling properties. The theoretical sensitivities were evaluated based on the parameters extracted from the experimental data. We report here, a fabricated Monolithic Microwave Integrated Circuit (MMIC) detector composed of a 6×6 μm^2 zero-bias tunnel diode and matching network to detect an RF signal ranges from 4 to 18 GHz. The circuit provides a voltage sensitivity of 3650 V/W and NEP of 5.5 pW/$\sqrt{Hz}$ at 11 GHz. The integrated GaAs/AlAs ASPAT detector with its input and output coplanar-waveguide (CPW) feeding can be easily incorporated into GaAs microwave circuits. The work reported here demonstrates an ASPAT detector model designed and optimized with the help of harmonic balance analysis (HBA) tool embedded in advanced design system (ADS) software. The validated model represents a platform that can be extended to design and realize high frequency detectors. For full circuit implementation, it is crucial to employ diodes with superior DC and RF characteristics, in addition to incorporating highly advanced technology capable of micro scale circuits manufacturing. A reduction in the parasitic effects of passive components is the main interest of researchers, as these degrade the circuit performance by reducing the output voltage or shifting the resonance frequency. An optimized and robust epi-layer structure is also another factor to be considered to mitigate any variations with device performances due to change in nominal parameters such as doping profile or layers thickness. A high current density obtained in our tunnel diode when compared with the multi-barrier structures reported in [8] and [24], due to the high tunneling probability of single barrier device.

2 ASPAT Detector Performances

The core of integrated detector as shown in Fig. 1 consists of a single zero-bias ASPAT detector grown and fabricated as stated in [23]. Inclusive analysis of the device including growth process, effect of layer parameters on series resistance, comparison between two modeled structures with fabricated one was presented. Additionally, the measured and modeled I-V characteristics of different structures showing the tunnelling effect were also extensively studied and highlighted. Moreover, the work in [23], highlighted the impact of spreading distance between the anode and cathode terminals on the overall series resistance of the device. A large separation reduces the fringing capacitance introduced between the contacts but comes with the cost of a higher series resistance, hence deteriorates the cut-off frequency of the ASPAT diode. The fact that separation gap distance of 1 to 2 μm is limited by the optical lithography technology used. Various devices were modeled and optimized at our labs including high electron mobility transistors (HEMTs), heterojunction bipolar transistors (HBTs), PIN diodes, and avalanche photodiodes (APDs) [24], [25], [26], [27], [28], [29] to evaluate the impact of separation distance on the yield process and the losses in the bottom ohmic layer. The GaAs/AlAs ASPAT diode developed in this work has a separation distance of 1.5 μm. A semi-insulating 620 μm thick GaAs substrate was used and the growth process of the diode stack layers were performed utilizing a RIBER V100 HU Solid Source Molecular Beam Epitaxy (SSMBE) system. This work also is devoted to designing and optimizing a matching network using the layout tool embedded in ADS software with momentum simulation routine, where the coupling effect of the surrounding electromagnetic field of the fully integrated structure is taken into account. The performance of detector circuits relies on the optimization routine followed throughout the modeling procedure. The design of the detector involves determining the diode impedances at the desired RF frequency and input power level. Of note, the diode impedance value is critical and

dependent on the input power level. As such might contribute to a very large or very small diode impedance at a particular power level, that is a challenge to put in place an effective matching circuit capable of delivering most of the incoming power from the source into the two-terminal device. In this work, the diode impedance was obtained at 10 GHz and -27 dBm RF power and found to be $(19 - j316\ \Omega)$.

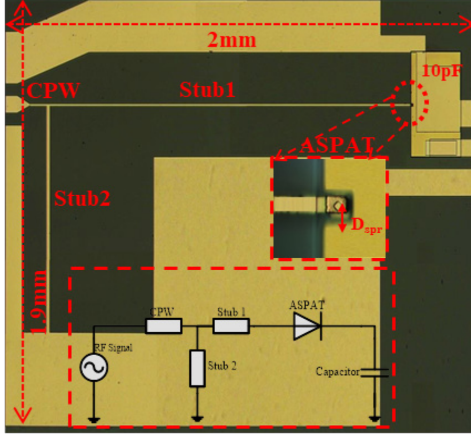

Fig 1. Fabricated 6×6 μm² ASPAT detector, inset is the schematic design. (Note: the image is not to scale).

Large imaginary part results in large matching stub size. Therefore, a tuning process was performed to optimize the transmission line stubs while keeping the die size as small as possible. The realization of the whole detector was successfully accomplished using the high-technology facilities at the university which include a class 1000 clean room equipped with i-line photolithography and deposition tools. Fig. 2 shows the measured current density and calculated curvature coefficient (K_v) of the discrete device under bias from -0.4 to 0.4 V.

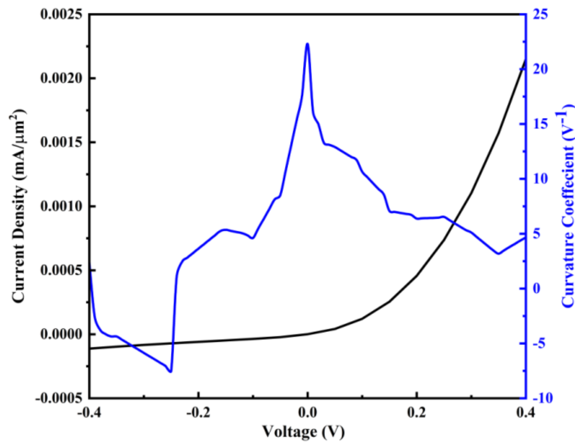

Fig 2. Measured current density and K_v of the 6×6 μm² ASPAT diode.

The forward current can be precisely adjusted by choosing the AlAs barrier thickness. It is evident that the curvature coefficient changes with the DC supply voltage and reaches its maximum level of roughly 22 V^{-1} at zero voltage, demonstrating the outstanding characteristic of the proposed diode. In [11], a 1×3 μm² low barrier diode with K_V of 24 V^{-1}, and R_S of 45 Ω at zero-bias voltage accommodating two frequency bands of 75 to 110 GHz and 140 to 220 GHz was described. A 2×2 μm² zero-bias Sb-Heterostructure diode reported in [30] has a K_v and R_S of 23 V^{-1} and 38 Ω, respectively. These paremetrs are very close to our obtained data although for smaller mesa area device in [11] and [30] and a thinner AlSb barrier is used [30]. In [31], a 0.8×0.8 μm² zero-bias GaAsSb/InAlAs/InGaAs tunnel diode with a K_v of 20 V^{-1}, R_J of 8 MΩ, and R_S of 130 Ω at room temprature and zero bias-voltage was used to cover the frequency band 200-340 GHz. The calculated NEP of the detector ranges between 125 to 270 pW/√Hz and this is due to its very large R_J. At 17K, K_v was decreased to 14 V^{-1} and R_J was increased to 23 MΩ, which undoubtedly would lead to a deterioration of the noise perfromance of the detector. Evidently, the reported K_v values are comparable to the ASPAT characteristics and indicate that optimizing the device mesa size and AlAs barrier thickness would improve the non-linear characteristics of the device even further. Indeed, many parameters should be considered for the purpose of implementing high-frequency detectors. The junction resistance, R_J is one of the crucial parameters that has a significant impact on the time response and noise performance of the whole system. Other key parameters are R_S and C_J which control the upper limit of the high-frequency operation. For mm-wave/THz detector, R_S and C_J are reduced to a few femto farads and ohms respectively to maximize the cut-off frequency. A high voltage sensitivity is also required as linked with high K_v achieved by decreasing the doping concentarion of the layers as was suggested in [32]. However, this would inevitably increase the contact resistance and degrade the high switching speed of the device.

In real-world circuit, two key features are paramount in evalulating detector perfromance including voltage sensitivity and NEP. The estimated voltage sensitivity reported in [31], [33], [34] were inaccurately derived, as it merely relies on the discrete device structure. However, the expression stated in Eq. (1) [35], [36] has been dedicated to consider additional parameters (i.e: junction resistance (R_J), K_v, and reflection coefficient).

$$S_{V_{actual}} = \frac{K_v R_J R_L (1-|\Gamma|^2)}{2(R_J+R_L)\left(1+\left(\frac{R_S}{R_J}\right)\right)^2 \left(1+\frac{\omega^2 C_J^2 R_S R_J}{1+\left(\frac{R_S}{R_J}\right)}\right)} \quad (1)$$

$(1-|\Gamma|^2)$ reflects the normalized power absorbed by the device, ω is the angular frequency and R_L is the load resistance. R_S, R_J, and C_J represents the device parameters extracted from RF measurements. All devices used in this work were fabricated in one and two ports configurations, and then characterised using on-wafer S-parameter measurements from 0.04 to 40 GHz. Short and open dummy structures were fabricated and tested as well, utilizing for a two-step de-embedding technique [37], [24] to eliminate the effect of the parasitic capacitance (C_P) and inductance (L_P) elements from the actual device. The measured one and two ports S-parameter data were fitted to the simulated S-parameter from the equivalent circuit model using ADS tools. For the verification of diode parameters, R_s and C_J were directly extracted from the measured S_{11} data utilizing the given formulas [38]:

$$R_S = real(-1/Y_{12}) \quad (2)$$

$$C_{total} = -imag(Y_{12})/\omega \quad (3)$$

C_{total} stands for the total capacitance including C_J and C_P. Comparable results were obtained for both equivalent circuits, which in-turns enable further verifying hence accurate parameters extraction. Moreover, R_J was obtained from the I-V characteristics and it agrees well with the one extracted from S-parameters as depicted in Fig. 3. More details on the methods used to extract diode parameters from measured S_{11} was demonstrated in [22] and [39]. The extraction procedure yields the following parameters: $R_{J@zero-bais}$=27 kΩ, $C_{J@zero-bias}$=49 fF, R_S=13 Ω, C_P= 16 fF and L_P=45 pH. The maximum cut-off frequency was evaluated and found to be 250 GHz. Accordingly, the device can be well-switching at the desired frequency band (4-18 GHz), without a degradation in the detector performance.

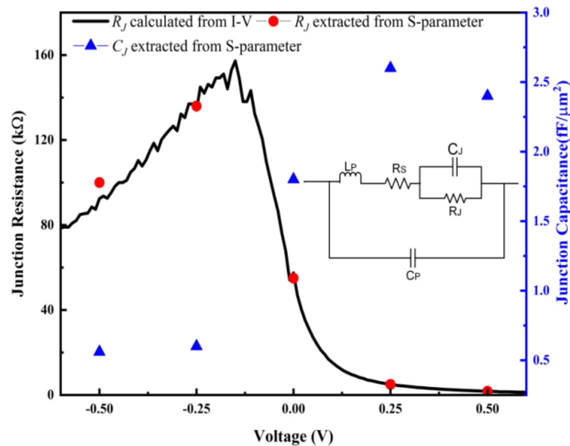

Fig 3. Extracted and calculated parameters of 6×6 μm² ASPAT diode. R_J is extracted from measured I-V and bias-dependent S-parameters. C_J and R_S are extracted from bias-dependent S-parameters.

An equivalent circuit model has been widely employed in different reported works [40], [41], [42] due to its simplicity and accuracy for application below 100 GHz. Nevertheless, a conventional circuit model does not provide an accurate extraction of diode parameters for RF measurements >100 GHz because of associated mm-wave signal losses. As such comes from electromagnetic interaction among surrounding components occurs at high frequency bands. A variable input power signal in terms of power and frequency was obtained from an Anritsu VNA and adjusted with an attenuator. Two steps were performed, first; the RF power was fixed at -27 dBm, whereas the frequency swept from 4 to 18 GHz as depicted in Fig. 4, second; the frequency was fixed at 11 GHz and the RF power was varied from -27 to -5 dBm as shown in Fig. 5. In both cases, the level of the RF power was precisely measured using Anritsu ML2430A . An accurate calibration technique was performed at each power level and frequency to remove the non-linear effect of the measurement equipment which could cause undesired power reflection.

For measurements of DC output voltage, a digital voltmeter with a high input impedance of 1 MΩ was utilized. Fig. 4 shows a good correlation between the measured and simulated data from 4 to 18 GHz. However, there is a small shift (around 4%) in the resonant frequency as can be attributed to the difference in the impedance matching conditions or due to the trivial error from measurements and other small parasitic contribution which are not considered in the simulation process. To sum up, the developed model presents a well-designed platform that can be used to predict the performance of proposed circuits for cost-effective manufacturing processes. The detector provides a moderate voltage sensitivity (S_v) of about 250 V/W at 4 GHz and increasing to a maximum level of ~3650 V/W at -27 dBm RF power and 11 GHz.

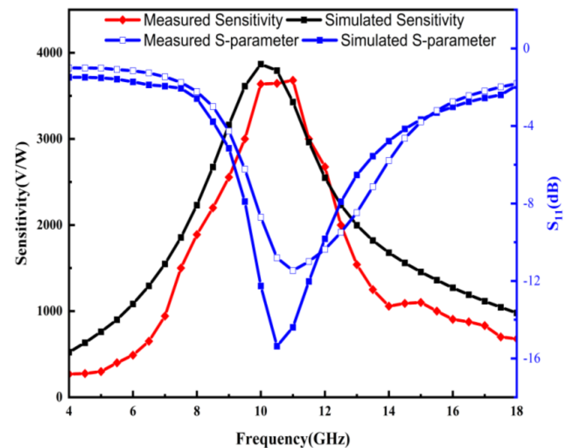

Fig 4. S_{11} reflection and sensitivity data of the detector at -27 dBm RF power.

This is higher than the reported value of our previous work in [43], where a voltage sensitivity of 1300 V/W was achieved at 24 GHz. The variation of detector output voltage with respect to RF power is shown in Fig. 5. For input power <-15 dBm, the detector has linear characteristics, however, the simulated output voltage deviates from the measured one at RF power >-15 dBm. This is mainly attributed to a mismatching issue as the circuit was developed to function at an RF power of <-15 dBm. The maximum measured output voltage is 319 mV at -4 dBm RF power, corresponding to a voltage sensitivity of 801 V/W. A high voltage sensitivity can be attainable from a sub-micrometer scale feature size and/or high curvature coefficient for efficient mm-Wave/THz frequency regime detector systems. NEP of the detector was evaluated using the expression ($\sqrt{4kTR_J}/S_{V_{actual}}$), where $S_{V_{actual}}$, k, and T are the measured voltage sensitivity, Boltzmann constant, and device temperature, respectively. The calculated NEP of the detector is 5.5 pW/$\sqrt{\text{Hz}}$.

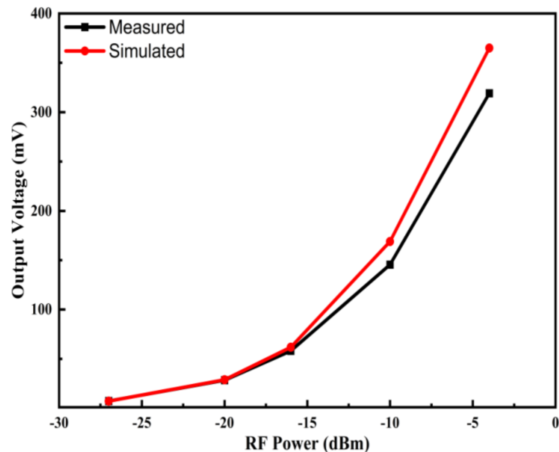

Fig 5. DC output voltage as a function of RF power at 11 GHz of the detector.

Table 1 presents a comparison between the performances of the proposed detector and other reported detectors based on Schottky, Backward diodes, and tunnel diodes. The detectors reported here showed improved voltage sensitivity and comparable noise equivalent power to zero-bias Schottky detector reported in [44] and [45] at 12.4 and 11 GHz, respectively. This work has also better voltage sensitivity of 3650 V/W as opponent to the other commercial tunnel based detectors, where their voltage sensitivities of 500 and 800 V/W published in [46] and [47], respectively. Schottky device demonstrated in [48] has small R_s and C_J when compared to 6×6 µm² ASPAT diode. However, this diode requires a 0.8 V to deliver a voltage sensitivity of 712 to 1483 V/W at frequency band of 26-40 GHz. Furthermore, ASPAT diode exhibited a comparable equivalent circuit parameters to the zero-bias backward diode adopted in [49]. With optimizing the transmission line stubs, the performance of the circuit is enhanced at high-frequencies. A minimized R_J can also lead to additional reduction in the NEP value. The main feature of temperature insensitive operation still gives the tunneling based ASPAT device a superior advantage over various conventional structures in literature.

3 Conclusion

A detailed work of radio-frequency operation detector developed with a zero-bias tunnel diode was described, focusing on the analysis of the DC and RF parameter of the device at different bias voltages and RF frequencies. A matching network-based on transmission line stubs was incorporated in the detector circuit for better power transmission from the source to the diode. The measured and simulated performances including detector sensitivity, S_{11} reflection coefficient, and DC output voltage at various RF power are greatly matched in the frequency band 4 to 18 GHz. The highest recorded voltage sensitivity is 3650 V/W at -27 dBm and decreasing to 801 V/W when RF power reaches -4 dBm. A higher voltage sensitivity is attainable from a sub-micrometer scale ASPAT device combined with stronger non-linearity features at zero-bias operation. Further improvement in matching circuit performance could also play a pivotal role in the future high-frequency detection circuits.

Conflict of Interest

The authors declare no conflict of interest.

Author Contributions

Omar S. Abdulwahid: Conceptualization, methodology, software, validation, formal analysis, investigation, data curation, writing - original draft, writing - review & editing, and project administration, **Saad G. Muttlak**: Conceptualization, methodology, validation, resources, writing - original draft, writing - review & editing, and visualization, **J. Sexton:** methodology, investigation, validation, and visualization, **M.J. Kelly**: Validation, and data curation, **Mohamed Missous**: Supervision, Writing - review & editing, and funding acquisition.

Funding

This work is funded by the Engineering and Physical Sciences Research Council (EPSRC) under the EP/P006973/1 “Future Compound Semiconductor Manufacturing Hub”.

Informed Consent Statement

Not applicable.

Table 1. Comparison of the Proposed Detector with Other Technologies.

RF freq. (GHz)	R_S (Ω)	C_J (fF)	R_J (kΩ)	K_V (V^{-1})	S_V(V/W)	NEP (pW/$\sqrt{Hz}$)	Diode type	Reference
4-18	13	49	27	~22	~3650@ 11 GHz	~5.5	Zero-bias ASPAT	This work
12.4	N/A	N/A	1 to 2	N/A	~1000	4.6	Zero-bias Schottky	[44]
2-18	20	300	N/A	N/A	~3000@ 11	1.49	Zero-bias Schottky	[45]
2-18	N/A	N/A	N/A	N/A	500	N/A	Zero-bias tunnel diode	[46]
6-12	N/A	N/A	N/A	N/A	800	N/A	Zero-bias tunnel diode	[47]
26 to 40	6	2.66	N/A	N/A	712 to 1483	25 to 40	Biased Schottky	[48]
50	11	118	0.282	N/A	498	N/A	Zero-bias backward	[49]
85-90	10.7	30	N/A	N/A	2500	N/A	Zero-bias Schottky	[50]

Declaration of generative AI and AI-assisted technologies

The author(s) declare that no generative AI or AI-assisted technologies were used in the writing process of this manuscript.

Acknowledgment

The authors are grateful to the Royal Society for supporting this work through a Brian Mercer award to the EPSRC-through (EP/P006973/1 “Future Compound Semiconductor Manufacturing Hub”).

4 References

[1] A. Hirata *et al.*, "120-GHz-band millimeter-wave photonic wireless link for 10-Gb/s data transmission," *IEEE transactions on microwave theory and techniques,* vol. 54, no. 5, pp. 1937-1944, 2006.

[2] I. Iñiguez-De-La-Torre *et al.*, "Operation of GaN planar nanodiodes as THz detectors and mixers," *IEEE Transactions on Terahertz Science and Technology,* vol. 4, no. 6, pp. 670-677, 2014.

[3] S. Diebold *et al.*, "Modeling and simulation of terahertz resonant tunneling diode-based circuits," *IEEE Transactions on Terahertz Science and Technology,* vol. 6, no. 5, pp. 716-723, 2016.

[4] T. Kleine-Ostmann and T. Nagatsuma, "A review on terahertz communications research," *Journal of Infrared, Millimeter, and Terahertz Waves,* vol. 32, pp. 143-171, 2011.

[5] Z. Zhang, R. Rajavel, P. Deelman, and P. Fay, "Sub-Micron Area Heterojunction Backward Diode Millimeter-Wave Detectors With 0.18 pW/Hz$^{1/2}$ Noise Equivalent Power," *IEEE Microwave and Wireless Components Letters,* vol. 21, no. 5, pp. 267-269, 2011.

[6] J. Schulman, D. Chow, and D. Jang, "InGaAs zero bias backward diodes for millimeter wave direct detection," *IEEE Electron Device Letters,* vol. 22, no. 5, pp. 200-202, 2002.

[7] S.-Y. Park, R. Yu, S.-Y. Chung, P. Berger, P. Thompson, and P. Fay, "Sensitivity of Si-based zero-bias backward diodes for microwave detection," *Electronics Letters,* vol. 43, no. 5, pp. 295-296, 2007.

[8] S. Takahagi, H. Shin-ya, K. Asakawa, M. Saito, and M. Suhara, "Equivalent circuit model of triple-barrier resonant tunneling diodes monolithically integrated with bow-tie antennas and analysis of rectification properties towards ultra wideband terahertz detections," *Japanese Journal of Applied Physics,* vol. 50, no. 1S2, p. 01BG01, 2011.

[9] A. Semenov, O. Cojocari, H.-W. Hübers, F. Song, A. Klushin, and A.-S. Müller, "Application of zero-bias quasi-optical Schottky-diode detectors for monitoring short-pulse and weak terahertz radiation," *IEEE Electron Device Letters,* vol. 31, no. 7, pp. 674-676, 2010.

[10] C. Yao, M. Zhou, Y. Luo, and C. Xu, "Millimeter wave broadband high sensitivity detectors with zero-bias Schottky diodes," *Journal of Semiconductors,* vol. 36, no. 6, p. 065002, 2015.

[11] S. Nadar *et al.*, "High performance heterostructure low barrier diodes for sub-THz detection," *IEEE*

Transactions on Terahertz Science and Technology, vol. 7, no. 6, pp. 780-788, 2017.

[12] A. V. Badin, V. D. Moskalenko, and D. A. Pidotova, "Application of the Schottky diode as a detector of continuous terahertz radiation," in *Journal of Physics: Conference Series*, 2021, vol. 1862, no. 1: IOP Publishing, p. 012012.

[13] R. Yadav *et al.*, "State-of-the-art room temperature operable zero-bias Schottky diode-based terahertz detector up to 5.56 THz," *Sensors,* vol. 23, no. 7, p. 3469, 2023.

[14] H. Kamble, M. Salek, and Y. Wang, "Zero-bias Schottky Diode Power Detector for D-band," in *2023 16th UK-Europe-China Workshop on Millimetre Waves and Terahertz Technologies (UCMMT)*, 2023, vol. 1: IEEE, pp. 1-3.

[15] S. M. Sze and K. K. Ng, *Physics of semiconductor devices*. John wiley & sons, 2006.

[16] M. R. Abdullah, Y. Wang, J. Sexton, M. Missous, and M. Kelly, "GaAs/AlAs tunnelling structure: Temperature dependence of ASPAT detectors," in *2015 8th UK, Europe, China Millimeter Waves and THz Technology Workshop (UCMMT)*, 2015: IEEE, pp. 1-4.

[17] Y. Wang, M. R. R. Abdullah, J. Sexton, and M. Missous, "Temperature dependence characteristics of In0. 53Ga0. 47As/AlAs asymmetric spacer-layer tunnel (ASPAT) diode detectors," in *2015 8th UK, Europe, China Millimeter Waves and THz Technology Workshop (UCMMT)*, 2015: IEEE, pp. 1-4.

[18] J. Karlovský, "The curvature coefficient of germanium tunnel and backward diodes," *solid-state Electronics,* vol. 10, no. 11, pp. 1109-1111, 1967.

[19] P. Chahal, F. Morris, and G. Frazier, "Zero bias resonant tunnel Schottky contact diode for wide-band direct detection," *IEEE Electron Device Letters,* vol. 26, no. 12, pp. 894-896, 2005.

[20] R. T. Syme, M. J. Kelly, M. Robinson, R. Smith, and I. Dale, "Novel GaAs/AlAs tunnel structures as microwave detectors," in *Quantum Well and Superlattice Physics IV*, 1992, vol. 1675: SPIE, pp. 46-56.

[21] R. Syme, "Tunnelling devices as microwave mixers and detectors," *Philosophical Transactions of the Royal Society of London. Series A: Mathematical, Physical and Engineering Sciences,* vol. 354, no. 1717, pp. 2351-2364, 1996.

[22] K. Z. Ariffin *et al.*, "Investigations of asymmetric spacer tunnel layer diodes for high-frequency applications," *IEEE Transactions on Electron Devices,* vol. 65, no. 1, pp. 64-71, 2017.

[23] K. Z. Ariffin *et al.*, "Investigations of Asymmetric Spacer Tunnel Layer Diodes for High-Frequency Applications," *IEEE Transactions on Electron Devices,* vol. 65, no. 1, pp. 64-71, 2018.

[24] S. G. Muttlak, O. S. Abdulwahid, J. Sexton, M. J. Kelly, and M. Missous, "InGaAs/AlAs resonant tunneling diodes for THz applications: an experimental investigation," *IEEE Journal of the Electron Devices Society,* vol. 6, pp. 254-262, 2018.

[25] O. S. Abdulwahid, I. Kostakis, S. G. Muttlak, J. Sexton, K. Ian, and M. Missous, "Physical modelling of InGaAs–InAlAs APD and PIN photodetectors for> 25 Gb/s data rate applications," *IET Optoelectronics,* vol. 13, no. 1, pp. 40-45, 2019.

[26] S. G. Muttlak, I. Kostakis, O. S. Abdulwahid, J. Sexton, and M. Missous, "Low-cost InP–InGaAs PIN–HBT-based OEIC for up to 20 Gb/s optical communication systems," *IET Optoelectronics,* vol. 13, no. 3, pp. 144-150, 2019.

[27] M. Sadeghi, J. Sexton, C.-W. Liang, and M. Missous, "Highly sensitive nanotesla quantum-well Hall-effect integrated circuit using GaAs–InGaAs–AlGaAs 2DEG," *IEEE Sensors Journal,* vol. 15, no. 3, pp. 1817-1824, 2014.

[28] S. G. Muttlak, O. Abdulwahid, J. Sexton, and M. Missous, "InGaAs/AlAs Resonant Tunneling Diodes with Very High Negative Differential Conductance for Efficient and Cost-Effective mm-Wave/THz Sources," in *2019 12th UK-Europe-China Workshop on Millimeter Waves and Terahertz Technologies (UCMMT)*, 2019: IEEE, pp. 1-3.

[29] O. S. Abdulwahid, J. Sexton, I. Kostakis, K. Ian, and M. Missous, "Physical modelling and experimental characterisation of InAlAs/InGaAs avalanche photodiode for 10 Gb/s data rates and higher," *IET optoelectronics,* vol. 12, no. 1, pp. 5-10, 2018.

[30] H. Moyer *et al.*, "Optimization of sb-heterostructure diode for low noise detection," in *Device Research Conference Digest, 2005. DRC'05. 63rd*, 2005, vol. 1: IEEE, pp. 263-264.

[31] M. Patrashin *et al.*, "GaAsSb/InAlAs/InGaAs tunnel diodes for millimeter wave detection in 220–330-GHz band," *IEEE Transactions on Electron Devices,* vol. 62, no. 3, pp. 1068-1071, 2015.

[32] T. Takahashi, M. Sato, Y. Nakasha, and N. Hara, "Sensitivity Improvement in GaAsSb-Based Heterojunction Backward Diodes by Optimized Doping Concentration," *IEEE Transactions on Electron Devices,* vol. 62, no. 6, pp. 1891-1897, 2015.

[33] M. Hrobak, M. Sterns, M. Schramm, W. Stein, and L.-P. Schmidt, "Planar zero bias Schottky diode detector operating in the E-and W-band," in *2013 European Microwave Conference*, 2013: IEEE, pp. 179-182.

[34] T. Takahashi, M. Sato, T. Hirose, and N. Hara, "Energy band control of GaAsSb-based backward diodes to improve sensitivity of millimeter-wave detection," *Japanese Journal of Applied Physics,* vol. 49, no. 10R, p. 104101, 2010.

[35] R. Syme, "Microwave detection using GaAs/AlAs tunnel structures," *GEC journal of research,* vol. 11, no. 1, pp. 12-23, 1993.

[36] V. I. Shashkin *et al.*, "Millimeter-wave detectors based on antenna-coupled low-barrier Schottky diodes," *International journal of infrared and millimeter waves,* vol. 28, no. 11, pp. 945-952, 2007.

[37] M. Koolen, J. Geelen, and M. Versleijen, "An improved de-embedding technique for on-wafer high-frequency characterization," in *Proc. Bipolar Circuits Technol. Meeting*, 1991: Minneapolis, MN, pp. 188-191.

[38] U. R. Pfeiffer, C. Mishra, R. M. Rassel, S. Pinkett, and S. K. Reynolds, "Schottky barrier diode circuits in silicon for future millimeter-wave and terahertz applications," *IEEE Transactions on Microwave Theory and techniques,* vol. 56, no. 2, pp. 364-371, 2008.

[39] O. Abdulwahid, S. Muttlak, J. Sexton, M. Missous, K. W. Ian, and M. Kelly, "2 nd Subharmonic mixer based asymmetric spacer tunnel diode (ASPAT)," in *2017 10th UK-Europe-China Workshop on Millimetre Waves and Terahertz Technologies (UCMMT)*, 2017: IEEE, pp. 1-4.

[40] A. Y. Tang, V. Drakinskiy, K. Yhland, J. Stenarson, T. Bryllert, and J. Stake, "Analytical extraction of a Schottky diode model from broadband S-parameters," *IEEE transactions on microwave theory and techniques,* vol. 61, no. 5, pp. 1870-1878, 2013.

[41] B. N. Wesling *et al.*, "Extraction of small-signal equivalent circuit for de-embedding of 3D vertical nanowire transistor," *Solid-State Electronics,* vol. 194, p. 108359, 2022.

[42] Q. Liu, "Tunnel Diode/Transistor Integrated Circuits," University of Notre Dame, 2006.

[43] O. Abdulwahid, S. G. Muttlak, J. Sexton, M. Missous, and M. Kelly, "24Ghz zero-bias asymmetrical spacer layer tunnel diode detectors," in *2019 12th UK-Europe-China Workshop on Millimeter Waves and Terahertz Technologies (UCMMT)*, 2019: IEEE, pp. 1-3.

[44] K. Technologies, "423B, 8470B, 8472B, 8473B/C Low Barrier Schottky Diode Detectors."

[45] H. Wu, Y. Li, and L. Sun, "Design of 2-18GHz zero-bias Schottky diode detector," in *2019 International Applied Computational Electromagnetics Society Symposium-China (ACES)*, 2019, vol. 1: IEEE, pp. 1-2.

[46] https://www.pasternack.com/. Tunnel Diode Zero Bias Detector, SMA, 5 nsec Pulse Risetime, Positive Video Out, +17 dBm max Pin, 2 GHz to 18 GHz [Online] Available: https://www.pasternack.com/tunnel-diode-detector-sma-positive-2-18-ghz-pe80t6007-p.aspx

[47] E. Microdevices. 6.0-12.0 GHz Planar Tunnel Diode Detector DT6012A3 [Online] Available: https://www.eclipsemdi.com/product/dt6012a3-6-0-12-0-ghz-planar-tunnel-diode-detector/

[48] J. Mou, X. Lv, Y. Yuan, and W. Yu, "Ka-band quasioptical detectors based on antenna-integrated planar Schottky diodes," *Microwave and Optical Technology Letters,* vol. 53, no. 9, pp. 2019-2022, 2011.

[49] E. T. Croke *et al.*, "New tunnel diode for zero-bias direct detection for millimeter-wave imagers," in *Passive Millimeter-Wave Imaging Technology V*, 2001, vol. 4373: SPIE, pp. 58-63.

[50] C. Yao and Z. Sheng-Wei, "Design of millimeter-wave detectors based on zero-bias Schottky diode for direct detection system of CubeSat radiometer," *Journal of Infrared and Millimeter Waves,* vol. 41, no. 1, pp. 285-293, 2022.

Biographies

Omar Abdulwahid obtained his Bachelor's degree in Electronics Engineering and a Master degree in electronic and communication engineering from the University of Mosul in 2010 and 2013 respectively. In 2019, he completed his PhD degree in Electrical and Electronic Engineering from the University of Manchester. During the PhD study, he focused on the modelling and fabrication of millimetre

and sub-millimetre wave zero-bias detectors based (ASPAT). Moreover, he works on the physical modeling of the high-speed PIN and APD photo-detector diodes for the upcoming Fibre-To-The-Home (FTTH) and high-speed rack to rack communications systems. Currently, he is working as a lecturer in the department of Mechatronics Engineering at the University of Mosul-Iraq.

Saad G. Muttlak received his B.Sc. degree in Electrical Engineering from Tikrit University in 2003 and M.Sc. in Electronics and Communications from the University of Mosul in 2012 followed by an academic career as a lecturer at Tikrit University for two years. Since then, he has been pursuing his PhD degree from the Electrical and Electronic Engineering Department at the University of Manchester until 2020. Dr. Muttlak is currently a lecturer at the University of Tikrit, and he authored and co-authored over 20 papers in both journals of repute and conference proceedings. His research interests mainly focus on modeling and measurements of high-frequency front-end amplifier MMIC circuits, mm-wave/THz regime emitters/detectors, optoelectronic IC receivers for >10Gb/s data rate communication systems and miniaturized rectenna design for biomedical and industrial applications. Dr. Muttlak gathered experience research in academic and recently in industrial environment.

James Sexton received his bachelor's degree in electronic engineering from UMIST, in 2001, followed by his PhD in 2005. In the same year, he became a Research Associate at University of Manchester (UoM) developing high-speed, low-power digital front-end technology for the Square Kilometer array (SKA) and later for the Electro Magnetic Remote Sensing (EMRS) Defense Technology Centre (DTC). Since 2010, he has been the experimental officer of the III-V compound semiconductor fabrication facility at UoM. His current research interests include magnetic Hall Effect sensors, Resonant Tunneling Diodes (RTDs) and asymmetric spacer-layer tunnel (ASPAT) diodes.

Professor Michael Kelly has been Emeritus Prince Philip Professor of Technology at the University of Cambridge since 2016. His MSc (1971) from Victoria University of Wellington, PhD (1974) from Cambridge University and post-doc until 1981, member of research staff of GEC (1981-1992, took two families of microwave devices form the laboratory into production), Professor at University of Surrey (1992-2002), and Cambridge 2002-16. He is a Fellow of the Royal Society of London, the Royal Academy of Engineering and Honorary Fellow of the Royal Society of New Zealand.

Mohamed Missous, FREng, FInstP, FIET, SMIEEE, is Professor of Semiconductor materials and Devices in the School of Electrical and Electronic Engineering at the University of Manchester. His research activities are centered on the growth of complex multi-layer semiconductor films by the technique of Molecular Beam Epitaxy (MBE). He has established a large MBE and Compound Semiconductor laboratory for materials growth, assessment equipment, compound semiconductor processing facility and device testing. Over the years he has concentrated, with considerable success, on establishing practical approaches and techniques required to meet stringent doping and thickness control, to sub monolayer accuracy, for a variety of advanced quantum devices, from room temperature operating mid infrared quantum well infrared photo-detectors, NanoTesla magnetic imaging using ultra-sensitive 2DEG for Non-Destructive Testing, 77 GHz car radars to Terahertz materials for 1.55 µm imaging. He now concentrates on the manufacturability of quantum devices including tunnel structures. Together with Professor Mike Kelly he was awarded the 2015 Royal Society Brian Mercer award for manufacturability of tunnel devices. He is regularly invited to give talks at international venues on mm-wave and THz technologies. His involvement in the above research topics has led to the publication of more than 240 papers in the open, international literature.